INL/CON-12-26774
PREPRINT

Electrochemistry of LiCl-Li_2O-H_2O Molten Salt Systems

2013 TMS Annual Meeting & Exhibition

Natalie Gese
Batric Pesic

March 2013

The INL is a
U.S. Department of Energy
National Laboratory
operated by
Battelle Energy Alliance

ELECTROCHEMISTRY OF LiCl-Li_2O-H_2O MOLTEN SALT SYSTEMS

Natalie Gese[1] and Batric Pesic[2]

[1]Idaho National Laboratory, Separations Department,
Nuclear Science and Technology Directorate;
P.O. Box 1625-6180; Idaho Falls, ID 83415, USA
[2]University of Idaho, Chemical and Materials Engineering Department;
Moscow, ID 83844-3024, USA

Molten Salt, Electrochemistry, Electrolytic Reduction, Electrorefining, Spent Fuel

Abstract

Uranium can be recovered from uranium oxide (UO_2) spent fuel through the combination of the oxide reduction and electrorefining processes. During oxide reduction, the spent fuel is introduced to molten LiCl-Li_2O salt at 650°C and the UO_2 is reduced to uranium metal via two routes: (1) electrochemically, and (2) chemically by lithium metal (Li°) that is produced electrochemically. However, the hygroscopic nature of both LiCl and Li_2O leads to the formation of LiOH, contributing hydroxyl anions (OH^-), the reduction of which interferes with the Li° generation required for the chemical reduction of UO_2. In order for the oxide reduction process to be an effective method for the treatment of uranium oxide fuel, the role of moisture in the LiCl-Li_2O system must be understood. The behavior of moisture in the LiCl-Li_2O molten salt system was studied using cyclic voltammetry, chronopotentiometry and chronoamperometry, while reduction to hydrogen was confirmed with gas chromatography.

1. Introduction

Oxide reduction is the key process used to convert spent oxide fuel to metal suitable for treatment in an electrorefiner [1, 2, 3]. During the reduction process, oxide fuel is converted to metal electrolytically and chemically in a vessel containing electrolyte comprised of molten LiCl-Li_2O at 650°C [4, 5]. Conversion efficiencies of 99.7% (for the conversion of oxide to metal) and enhanced reduction rates (due to the fast kinetics of lithium reduction from Li_2O) have been reported [6, 7]. In the electrorefining process, remaining fission products, transuranics and minor actinides are separated to yield a high purity uranium metal product (>99.99%) [6, 7]. One of the major causes of lower current efficiencies in the oxide reduction process is attributed to the recombination of lithium with oxygen in the cell and the decrease in oxide ion concentration from Li_2O degradation [15]. The results here will provide a fundamental understanding of the impact of moisture, and the mechanism and need to purify the molten salt, in order to achieve higher throughput for the oxide reduction process. It has been determined that moisture reacts with Li_2O to produce LiOH and, as a result, the reduction of OH^- ions produces hydrogen gas on the working electrode preferentially to lithium.

Electrochemical stability, reaction kinetics, and high ionic conductivities are among the favorable properties of LiCl based melts [8, 9, 10]. However, lithium chloride as well as other

lithium based salts will form hydrates [11]. LiCl crystallizes with water to form $LiCl{\cdot}H_2O$ and $LiCl{\cdot}1/2\ H_2O$, which have been reported to thermally decompose at 98-110°C and 152-162°C, respectively [12]. Moisture in LiCl and LiCl-KCl melts has been observed, even following many different moisture removal treatment methods [13, 14]. The choice of LiCl molten salt used for the oxide reduction process is due to the high solubility of Li_2O from which Li metal can be made in-situ for chemical reaction with UO_2. Counter electrode degradation is prevented in LiCl containing greater the 0.5 wt% Li_2O [15]. Advantages for transition to LiCl-Li_2O system from the LiCl-Li and LiCl-KCl based systems for oxide reduction have been discussed in detail elsewhere [16, 17, 18, 19, 20, 21, 22, 23, 24].

2. Experimental

The electrochemistry of the molten salt systems was studied in the range of 650 to 665°C. All experiments were carried out in ultra high purity argon atmosphere. Anhydrous lithium chloride (99.7%), Li_2O (99.5%), and LiOH (prepared from LiOH monohydrate) were purchased from Alfa Aesar. Ultra high purity LiCl (99.995%) was used as a control for the lower grade LiCl. The working electrode was made of 1-mm-dia. nickel or molybdenum. The counter electrode was made of 3-mm-dia, high purity graphite rod or 6-mm-dia. glassy carbon rod. A 0.5-mm-dia. molybdenum wire was used as a quasi-reference electrode (QRE) due to its consistent stability in the molten salt systems studied. In addition, molybdenum does not adsorb or form alloys with lithium, which is why it was chosen over platinum, which is known to react with lithium [25].

3. Results and Discussion

Cyclic voltammetry (CV) and chronopotentiometry (CP) were run at 665°C. According to the results of the CVs in Figure 1(a), the presence of 1 wt% Li_2O in LiCl caused a positive shift in the reduction potential of lithium ion by 0.8 V. The shift of reduction potential in LiCl-Li_2O was also confirmed by CP, as shown in Figure 1 (b). Because of highly hygroscopic nature of LiCl, and reactivity of Li_2O with water, it was decided to examine the effect of moisture on the cyclic voltammetry presented in Figure 1 (a-b). For that purpose, aliquot amounts of water were added to LiCl salts and the effect monitored was the development of a precurrent, which is defined as current developing prior to the onset of the main lithium ion reduction current as seen during cyclic voltammetry. It should be noted that, in our experimental conditions, precurrents were noticeable even with ultradry LiCl salts of 99.995% purity.

Hur et al. [7] found that the decomposition voltage of Li_2O is based on an activity coefficient of 8.4 for Li_2O in LiCl and on the measured solubility of 11.9 mol% (8.7 wt%) at 650°C. The reduction of lithium from LiCl-Li_2O (reaction (1)) can be expressed by the Nernst relationship (equation (2)) where $E°$ is the standard potential of an electrode, R is the gas constants, T is the temperature and F is the Faraday constant. The activity of metallic lithium (Li°) and lithium ions (Li^+) are given as $a_{Li°}$ *and* a_{Li+}, respectively.

$$Li^+ + e = Li° \qquad (1)$$

$$E = E° + RT/nF*ln(a_{Li+}/a_{Li°}) \qquad (2)$$

When more than a monolayer of lithium is deposited on a solid electrode at any given time, the activity for lithium, a_{Li°, can be assumed to be equal to 1 and, consequently, $E = E^\circ$. However, when there is less than a monolayer of lithium deposited on the surface of the electrode, the activity of lithium is not equal to 1, $a_{Li^\circ} \neq 1$. For the latter case, lithium deposition will begin at underpotential, which are potentials more positive than values where deposition of lithium occurs on pre-deposited lithium [7]. Therefore, when lithium is reduced and then dissolved into the melt, the electrode surface is continuously in the $a_{Li^\circ} \neq 1$ state and lithium underpotential deposition (UPD) will occur.

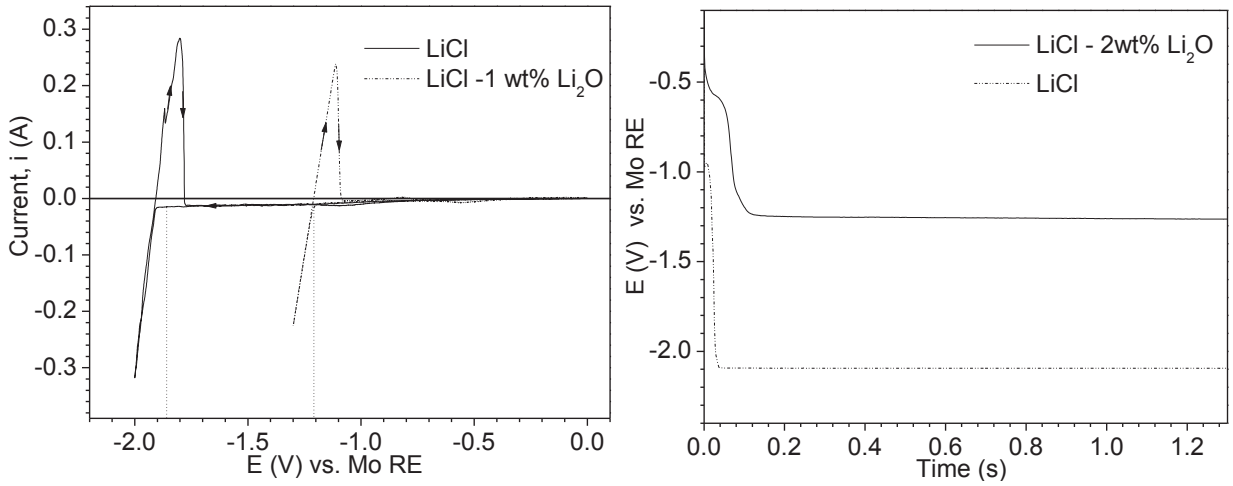

Figure 1. Lithium reduction from LiCl and LiCl-Li_2O molten salts at 650°C characterized by (a) CV at 20 mV/s scan rate, and (b) by CP at 100 mA imposed current. Conditions: WE(Ni), QRE(Mo), CE(glassy carbon).

It has been observed that when lithium is generated in LiCl molten salt systems, black fog is evolved from the surface of the electrode in regions more positive than the lithium reduction potential. To confirm that black fog is produced from lithium metal, a bead of pure lithium was added to LiCl-Li_2O molten salt. On contact with the salt, black fog was produced as the lithium metal dissolved into the salt. It is well known that atomized metal will appear as black streams in clear molten salts. Therefore, the streams of black fog evolved from the electrode surface during electrochemically reducing conditions, in the three molten salt systems studied, may be attributed to UPD of lithium.

The effect of scan rate was also studied in the LiCl-Li_2O molten salt system, Figure 2(a). There are two reactions which may contribute to the precurrent observed prior to the onset of lithium reduction (1) UPD of lithium and (2) reduction of OH^- ions. CVs run at less than 1 V/s were independent of scan rate. Above 1 V/s, the precurrent observed prior to the onset of lithium reduction became more pronounced. The reaction between hydrogen produced at the working electrode from the reduction of OH^- with UPD lithium is fast and cannot be resolved by CVs run at less than 1 V/s. Therefore, scan rates were extended beyond 10 V/s to resolve the scan rate dependencies of these reactions. Figure 2(b) shows the Randles–Sevčik relationship between the peak current values versus the square root of scan rate. There are two scan rate regions represented in this plot, (1) 0-10 V/s and (2) 10-100 V/s. The data for the second region can be

extrapolated through the origin. The linear behavior indicates a reversible reaction system and the diffusion coefficient can be calculated from the Randles-Sevčik relationship (equation (3)) at 650°C, where, n = the number of electrons, A = the electrode surface area (cm^2), C_i = the concentration of OH^- ($moles/cm^2$), v = scan rate, and D = the diffusion coefficient (cm^2/s).

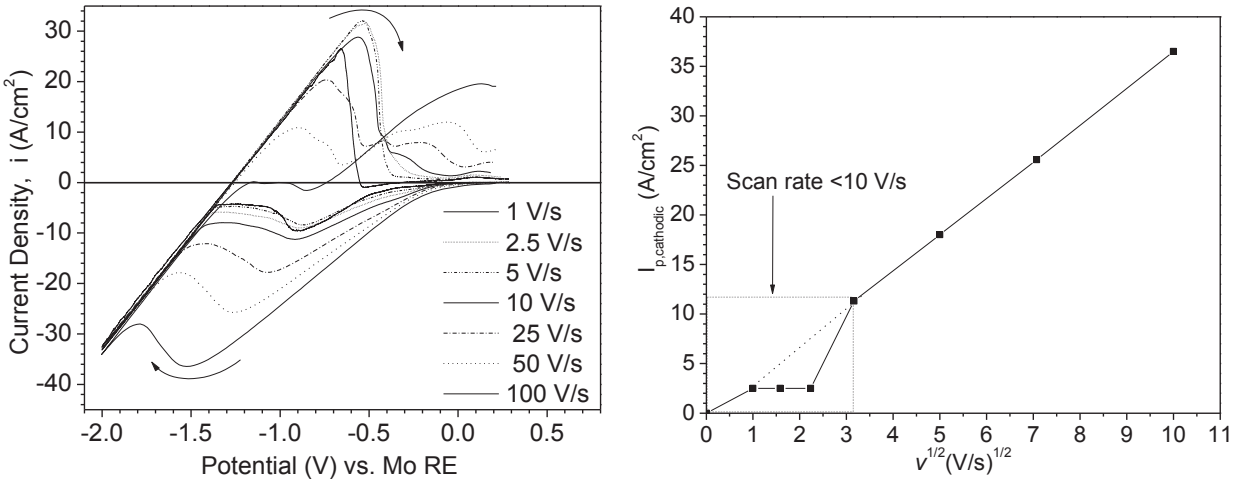

(a) (b)

Figure 2. (a) Effect of scan rate on CV of LiCl - 2wt% Li_2O molten salt at 665 °C, and (b) Corresponding Randles-Sevčik plot. Conditions: WE(Ni), QRE(Mo), CE(glassy carbon).

$$I_p = -1.53 \times 10^5 \cdot n^{3/2} A \cdot D^{1/2} \cdot C_i \cdot v^{1/2} \qquad (3)$$

It is speculated that the reactions being observed at scan rates greater than 10 V/s are OH^- (LiOH) reduction to produce hydrogen (reaction (4)), which then proceeds to form LiH (reaction (5)). The LiH is very stable at the temperature used for these experiments and the currents observed in the pre-lithium reduction range are likely produced by both the reduction of lithium and H_2 gas evolution [26]. In addition, LiH and LiOH can react to form Li_2O and H_2 gas (reaction (6)).

$$LiOH + e \rightarrow Li^+ + 1/2H_2 + O^{2-} \qquad (4)$$

$$Li^+ + 1/2H_2 + e \rightarrow LiH \qquad (5)$$

$$LiH + LiOH \rightarrow Li_2O + H_2 \qquad (6)$$

To show that the pre-peak currents are related to the presence of water in the molten salts, known amounts of H_2O were added to LiCl-Li_2O salt and known amounts of LiOH were added to LiCl salt and electrochemical measurements of each system were made. The formation of LiOH from reaction of Li_2O with H_2O in LiCl-Li_2O molten salt was confirmed by running CVs as a function of H_2O concentration shown in Figure 3(a). Controlled amounts of LiOH were added to LiCl to confirm that LiOH forms from interaction of Li_2O with hydrated LiCl. CV of LiCl-LiOH molten salt was used to compare to the CVs run in LiCl-Li_2O-H_2O system as shown in Figure 3(b). The concentration of LiOH was varied from 0.5 wt% to 2 wt%. The cathodic current increased with LiOH concentration. Excessive gas production on the working electrode was observed in addition to simultaneous production of black fog. For both the LiCl-Li_2O-H_2O and LiCl-LiOH

systems, bubbling was observed at the counter electrode, however, not to the extent that was observed to evolve off the working electrode. The same features were present for both LiCl-Li_2O-H_2O and LiCl-LiOH systems, therefore, demonstrating that the Li_2O containing LiCl salt formed LiOH when contaminated with moisture.

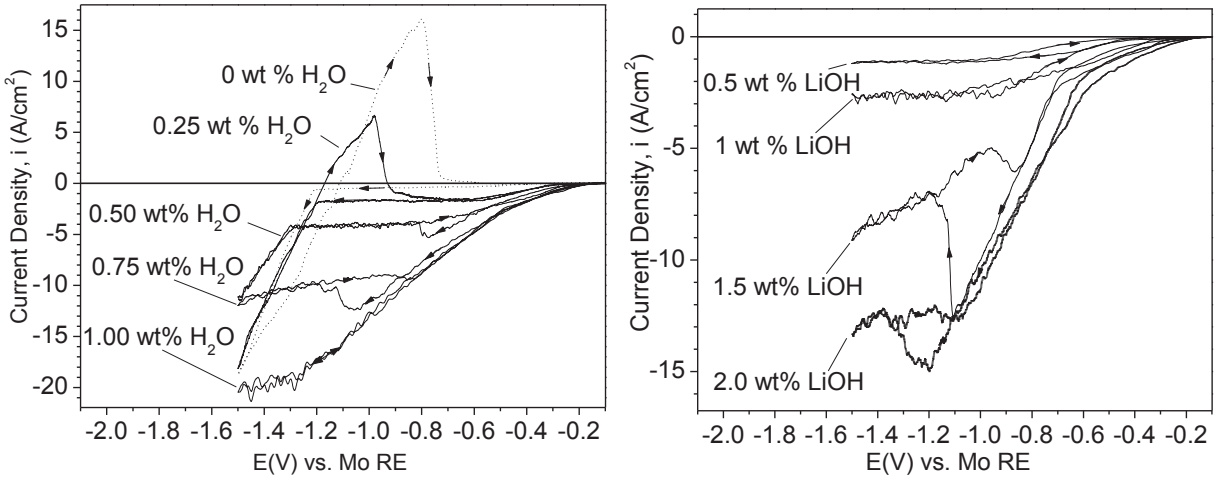

Figure 3. Effect of concentration of (a) H_2O on CV of LiCl-2wt% Li_2O, and (b) concentration of LiOH in LiCl, molten salts at 665 °C. Scan rate = 20 mV/s. Conditions: WE(Ni), QRE(Mo), CE(glassy carbon).

In both salt systems, LiCl-Li_2O-H_2O and LiCl-LiOH, the common feature was high bubbling rate of gas produced at the working electrode. The product was hydrogen gas as confirmed by gas chromatography (GC) in Figure 4. Based on the data presented in Figure 3(a) and (b), the following reaction scheme (reactions (5)-(8)), is proposed.

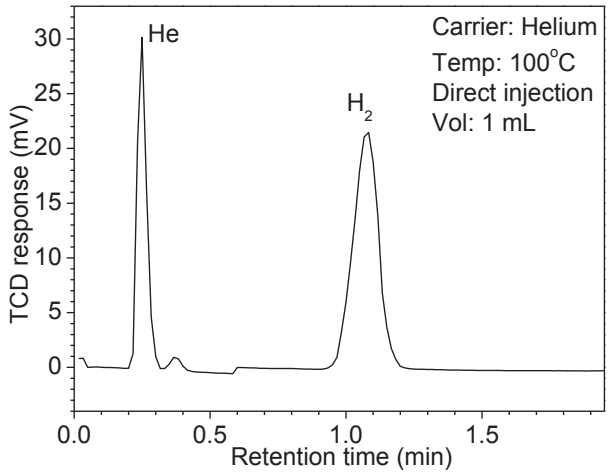

Figure 4. Gas chromatogram of gaseous reaction product collected at the working electrode during LiCl-LiOH electrolysis at 665°C.

In the salt, Li_2O reacts with H_2O to form LiOH (reaction (5)), which dissociates to Li^+ and OH^- (reaction (6)). The hydroxide ion reacts at the working electrode to produce hydrogen gas and oxide ion O^{2-} (reaction (7)). Lithium ions and oxide ions produced at the working electrode react

to regenerate Li_2O (reaction (8)). And, oxide ions that reach the counter electrode are oxidized to form oxygen gas (reaction (9)). The overall reaction (reaction (10)) is dissociation of water into hydrogen gas and oxygen, without any lithium produced.

Salt:

$Li_2O + H_2O \rightarrow 2LiOH$ (5)

$2LiOH \rightarrow 2Li^+ + 2OH^-$ (6)

Working electrode:

$2OH^- + 2e \rightarrow H_2 + 2O^{2-}$ (7)

Salt:

$2Li^+ + 2O^{2-} \rightarrow Li_2O + O^{2-}$ (8)

Counter electrode:

$O^{2-} \rightarrow 1/2O_2 + 2e$ (9)

$H_2O \rightarrow H_2 + 1/2O_2$ (10)

It is possible for moisture from the atmosphere to react with molten LiCl-Li_2O salt. To confirm this effect, 15 mL of water was allowed to stand inside the glovebox (425-L-vol. argon atmosphere) and the regeneration system for moisture removal was shut off. Cyclic voltammetry was run as a function of the time that the salt was exposed to the moisture containing atmosphere, Figure 5(a). An uptake of moisture in the salt after 8 hours of exposure was equivalent to the results with 0.75 wt% H_2O in the LiCl-2 wt% Li_2O salt at temperature of 650°C, shown in Figure 3(a), which corresponds to roughly 7500 ppm H_2O. In addition, CV was run as a function of the time that the salt was exposed to the standard dry-argon atmosphere in the glovebox as a control (Figure 5(b)), which shows that there was no uptake of moisture in the salt after 8 hours of exposure.

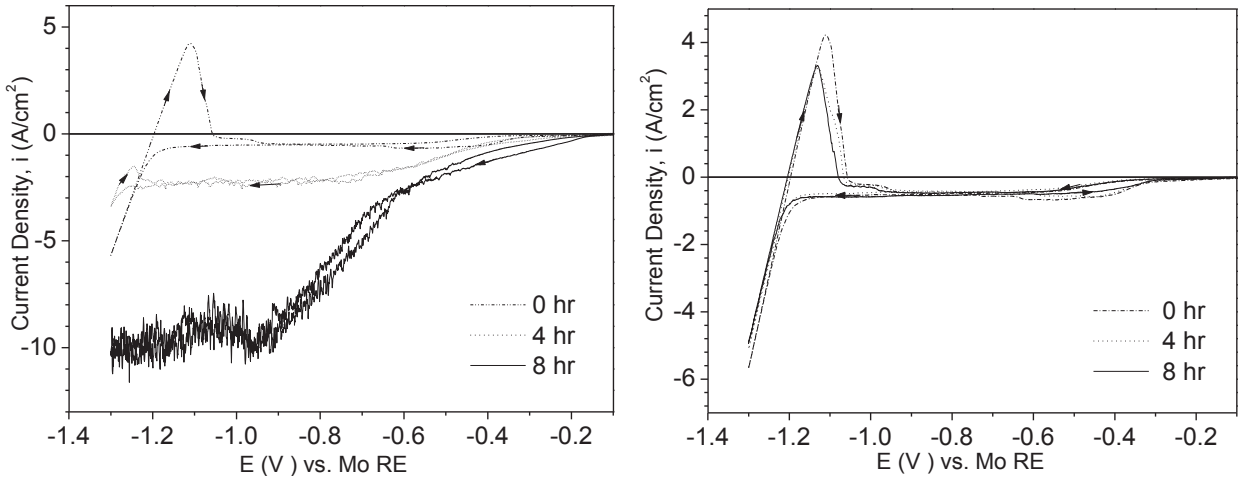

Figure 5. CV of LiCl-2wt% Li_2O at 665 °C as a function of time (a) exposed to argon containing moisture atmosphere and (b) ordinary argon atmosphere. Conditions: Scan rate = 20 mV/s. WE (Mo), QRE(Mo), CE(graphite).

Cyclic voltammetry as a function of the order in which Li_2O was added to hydrated LiCl salt was run to determine how moisture can enter and interfere with the LiCl-Li_2O salt system. In the first approach, water and LiCl salt were mixed at room temperature and subsequently heated to 665°C to melt the salt, upon which 1 wt% Li_2O was added to the melt. In the second approach, water, LiCl, and Li_2O were mixed at room temperature and subsequently heated to 665°C to melt the salt. Figure 6(a) shows the effect of the order of addition of Li_2O.

According to Figure 6(a), in the first approach, when Li_2O is charged into the LiCl subsequent to its melting, the formation of LiOH will not occur, resulting in a typical lithium reduction cyclic voltammogram. LiOH is not able to form because all of the added water evaporates during heating and melting of hydrated LiCl salt [27]. However, in the second approach, when Li_2O was added to hydrated LiCl at room temperature prior to melting, Li_2O reacts readily with the water to produce LiOH. As a consequence, its formation is responsible for significant precurrents, Figure 6(b). Similar cathodic precurrent has also been observed in other studies, indicating LiOH participation [28]. At 20 mV/s, on the scan reversal, the peak for lithium is absent, due to the consumption of lithium in a chemical reaction with hydrogen, which is produced simultaneously on the working electrode. At the faster scan rate, 500 mV/s, the lithium peak is observed because the reaction between lithium and hydrogen cannot occur fast enough to mask the presence of lithium on the electrode.

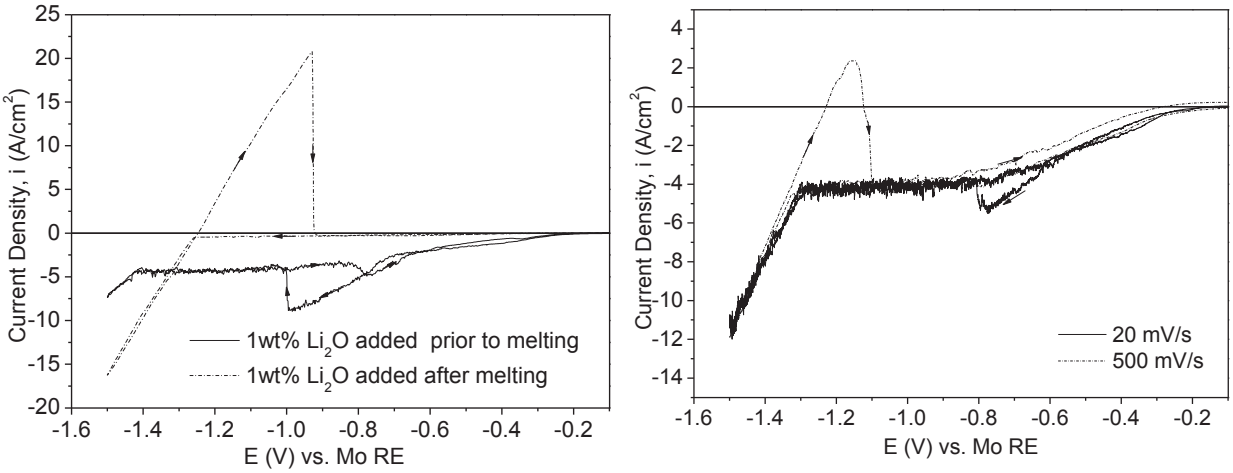

Figure 6. CV of LiCl-2wt% Li_2O as a function of order of addition of Li_2O to LiCl-0.5wt% H_2O salt at 665°C. (a) Addition of 2wt% Li_2O to LiCl-0.5wt%H_2O before (solid line), and after salt melting (dashed line). Scan rate = 20mV/s. (b) Effect of scan rate on CV when equivalent 2wt% Li_2O was added prior to melting of LiCl. Conditions: WE(Mo), QRE(Mo), CE (graphite).

4. Conclusions

1. Moisture contamination to the LiCl-Li_2O in the form of LiOH comes from (1) Li_2O interaction with hydrated LiCl, (2) Li_2O interaction with trace LiOH, and (3) the reaction of LiCl-Li_2O molten salt with moisture containing atmosphere.
2. The potential for reduction LiOH is more positive than the reduction potential of lithium. Therefore, there will always be currents preceding lithium reduction if moisture impurities

are present, complicating the practical application of these salts by overriding all pertinent electrochemical reactions.

3. In more cathodic regions, vigorous hydrogen gas bubbling purges Li metal away from the electrode surface, precluding its detection by anodic oxidation.
4. The reasons for the cathodic pre-currents in electrochemistry of LiCl-KCl and LiCl-Li_2O systems have not been studied before. More studies are required to elucidate the mechanisms responsible for these pre-currents.

5. References

1. Goff, K. M. and Simpson, M. F. (2009). Dry Processing of Used Nuclear Fuel.
2. Simpson, M. F. (2010). DOE Contract DE-AC07-05ID14517 INL/EXT-10-17753: 31.
3. Herrmann, S. D. and Li, S. X. (2010). Nuclear Technology 171(3): 247-265.
4. Herrmann, S. D., et al. (2002). ANS Fifth Topical Meeting. Charleston, S. C.
5. Jeong, S. M., et al. (2010). Nuclear Engineering and Technology 42(2): 183-192.
6. Herrmann, S. D. and Li, S. X. (2010). Nuclear Technology 171(3): 247-265.
7. Hur, J.-M., et al. (2010). Electrochemistry Communications 12(5): 706-709.
8. Poignet, J. C. and Fouletier, J. (2008). Materials Issues for Generation IV Systems: 523-536.
9. Orbakh, D. Nonaqueous Electrochemistry. New York: Marcel Dekker, 1999.
10. Kissinger, P. T. and Heineman, W. R. (1996). New York, Marcel Dekker, Inc.
11. Masset, P. and Guidotti, R. A. (2007). Journal of Power Sources 164(1): 397-414.
12. Voigt, W. and Zeng, D. (2002). Pure and Applied Chemistry 74(10): 1909-1920.
13. Burkhard, W. J. and Corbett, J. D. (1957). J. of the American Chem. Soc. 79(24): 6361-6363.
14. Tetenbaum, M. F., et al. (1985). Fusion Technology 7(1): 53-56.
15. Karell, E. J., et al. (2001). Nuclear Technology 136(3): 342-353.
16. Herrmann, S. D., et al (2002) Idaho Falls: 1-7.
17. Nakajima, T., et al. (1974). Bulletin of the Chemical Society of Japan 47(8): 2071-2072.
18. Nakanishi, K. (1970). Industrial & Engineering Chemistry Fundamentals 9(3): 449-453.
19. Karell, E. J., et al. (2001). Nuclear Technology 136(3): 342-353.
20. Li, S. X. and Herrmann, S. D. (2002). Journal of the Electrochemical Soc. 149(2): H39-H43.
21. Shin, Y., et al. (2000). Journal of Radioanalytical and Nuclear Chemistry 243(3): 639-643.
22. Usami, T., et al. (2002). Journal of Nuclear Materials 300(1): 15-26.
23. Park, B. H. and. Hur, J. M (2010). Korean J. of Chemical Engineering 27(4): 1278-1283.
24. Sakamura, Y. (2010). Journal of The Electrochemical Society 157(9): E135-E139.
25. Laitinen, H. A. Polarography in Molten Salts.
26. Nohira, T. and Y. Ito (2002). Journal of the Electrochemical Society 149(5): E159-E165.
27. Burkhard, W. J. and Corbett, J. D. (1957). J. of the American Chem. Soc.79(24): 6361-6363.
28. Park, B. H., I. W. Lee, et al. (2008). Chemical Engineering Science 63(13): 3485-3492.